Journal of Asian Earth Sciences 90 (2014) 157–172

Contents lists available at ScienceDirect

Journal of Asian Earth Sciences

journal homepage: www.elsevier.com/locate/jseaes

Holocene *versus* modern catchment erosion rates at 300 MW Baspa II hydroelectric power plant (India, NW Himalaya)

Erich Draganits [a,b,*], Susanne Gier [a], Christa-Ch. Hofmann [c], Christoph Janda [d], Bodo Bookhagen [e], Bernhard Grasemann [a]

[a] Department of Geodynamics and Sedimentology, University of Vienna, Althanstrasse 14, A-1090 Vienna, Austria
[b] Department of Prehistoric and Historical Archaeology, University of Vienna, Franz-Klein-Gasse 1, A-1190 Vienna, Austria
[c] Department of Palaeontology, University of Vienna, Althanstrasse 14, A-1090 Vienna, Austria
[d] Geological Survey of Austria, Neulinggasse 38, A-1030 Vienna, Austria
[e] Department of Geography, University of California Santa Barbara, 1832 Ellison Hall, Santa Barbara, CA 93106-4060, USA

ARTICLE INFO

Article history:
Received 19 February 2014
Received in revised form 15 April 2014
Accepted 16 April 2014
Available online 26 April 2014

Keywords:
Erosion
River load
Lake sediments
Palynology
Landslide-dammed lake

ABSTRACT

300 MW Baspa II is India's largest private hydroelectric facility, located at the Baspa River which is an important left-hand tributary to the Sutlej River in the NW Himalaya (India). In this valley the Sangla palaeo-lake has been dammed around 8200 yr BP behind a rock-avalanche dam and Baspa II is located exactly on top of this palaeo-lake. This special location represents a very rare possibility to evaluate the short-term, river load and hydrological parameters measured during the planning and operational stages of Baspa II with the long-term parameters gained from the palaeo-lake sediments from the catchment. Sedimentological and geomorphological investigations of the lacustrine sediments have been used to reconstruct environmental changes during >2500 years of its existence. The Mid-Holocene erosion rates of the Baspa catchment estimated from the volume and duration of deposition of the exposed lake sediments are at 0.7–1.0 mm yr^{-1}, almost identical with the modern erosion rates calculated from river gauge data from Baspa II. Several charcoal layers and charcoal pieces from the uppermost palaeo-lake levels around 5000 cal yr BP might be related to woodland clearance and they possibly represent one of the oldest evidences for human presence in the Baspa Valley during Neolithic time.

1. Introduction

Since Dahlen and Suppe (1988) have shown that erosion can influence tectonics, there has been ongoing discussion about the importance amongst themselves and variations in the interrelationship between tectonic movements, climate change and geomorphology (Molnar and England, 1990; Beaumont et al., 2001; Willett et al., 2006; Molnar, 2009; Whipple, 2009; Burbank et al., 2012; Whittaker, 2012). In the present study we compare modern erosion measurements from a Himalayan catchment with Early-Mid Holocene erosion rates estimated from the sediment fill of a mass-movement dammed palaeo-lake.

Natural dams resulting from large mass-movements are common features of mountain ranges which create engineering geological challenges and have an important impact on the geomorphological evolution of these areas (Schuster and Costa, 1986; Costa and Schuster, 1988, 1991; Hewitt, 2011; Korup, 2011; Weidinger, 2011). They have the potential to block even large rivers up to several thousands of years, forcing the upstream accumulation of water as well as sediment and may cause catastrophic outburst floods (Schuster and Costa, 1986; Costa and Schuster, 1991; Korup et al., 2006; Weidinger, 2011).

Consequently the damming of rivers by mass-movements affects several important geomorphological parameters of river networks including run-off characteristics, sediment budget, longitudinal profile and even river ecosystems (Mackey et al., 2011). Depending on the size and duration of river blockage, the impact of palaeo-lakes can be detected for a long time and geomorphological features including former shore lines, knick-points and lake sediments can be utilized for lake reconstruction.

The 300 MW Baspa II, India's largest private hydroelectric facility, was built on top of a relict Holocene rock avalanche-dam lake in the Baspa Valley in the NW Himalaya of India (Draganits et al., 2014). The period of instrumental seismic measurements is about 100 years and many hydrological and sedimentological measurements carried out in the planning stage and during the operation

* Corresponding author at: Department of Geodynamics and Sedimentology, University of Vienna, Althanstrasse 14, A-1090 Vienna, Austria. Tel.: +43 1 4277 53415; fax: +43 1 4277 9534.
E-mail address: Erich.Draganits@univie.ac.at (E. Draganits).

http://dx.doi.org/10.1016/j.jseaes.2014.04.016
1367-9120/

of Baspa II hardly cover more than 2 decades (JHPL, 2004; Wulf et al., 2012).

The whole lake volume of Sangla palaeo-lake has been completely filled with sediments, before the Baspa River started down-cutting of the lacustrine deposits. According to radiocarbon ages of organic remains in the lake deposits, the silting of the basin upstream of the rock avalanche dam lasted >2500 years and therefore the lake sediments represent an invaluable archive for the reconstruction of the palaeo-hydrology, catchment denudation rates (Bookhagen et al., 2005a; Pratt-Sitaula et al., 2007; Burbank et al., 2012), palaeo-climate (Chakraborty et al., 2006) and tectonic activity (Montenat et al., 2007; Draganits et al., 2014) in this part of the Himalaya. Consequently, this study aims to utilize the lacustrine sediments as an archive for long-term parameters relevant for the 300 MW Baspa II built on top of the Sangla palaeo-lake and to compare modern river load and hydrological parameters measured during the planning and operational stages of Baspa II with the long-term parameters reconstructed from the palaeo-lake sediments from the catchment.

2. Geological setting of Baspa II

2.1. Regional geology

The Sutlej Valley forms a natural cross-section perpendicular to the general trend of the Himalayas and exposes all tectonic units of the orogen with the Baspa River as one of its most important tributaries. The crustal-scale Main Central Thrust, which separates the Lesser Himalayan and the Higher Himalayan Crystalline, is the most important tectonic feature in the Indian part of the Valley (Fig. 1). Geochronological data show that the Main Central Thrust was active during the Early Miocene (Hodges, 2000). Subsequently, the thrust was folded in a prominent antiform–synform foldtrain typical for the whole Himalayan orogen and in this way exposes Lesser Himalaya rocks in large windows (Vannay et al., 2004).

Based on the Early Miocene age of deformation (Hodges, 2000) and the fact that the Main Central Thrust is folded, it is clear that the Main Central Thrust is inactive today and therefore cannot be responsible for active tectonics in this area including thermal springs, steep near-surface thermal gradients, deformed Quaternary sediments, and seismicity (Srikantia and Bhargava, 1998; Vannay et al., 2004).

A probable candidate for triggering active tectonics in the Sutlej Valley is the still on-going out-of-sequence extrusion of a wedge-shaped metamorphic massif, the Lesser Himalayan Crystalline Sequence, between a thrust at the base, the Munsiari Thrust, and a concurrent normal fault on the top, the Karcham Normal Fault (Vannay and Grasemann, 2001; Hager, 2003; Vannay et al., 2004; Draganits et al., 2014). The extensional deformation is not restricted to the base of the Higher Himalayan Crystalline, but is typical for the whole area east of Karcham (i.e. hanging wall above the Karcham Normal Fault). The brittle faults indicate an overall NE–SW to E–W extensional regime (Hager, 2003; Hintersberger et al., 2011).

The Baspa River originates in latest Precambrian meta-sediments and along its flow it transects from ESE to WNW lower Palaeozoic and again latest Precambrian meta-sediments with the Ordovician Kinnaur Kailash Granite intruded into the latter (Tripathi et al., 2012). The Sangla Detachment, the local equivalent of the South Tibetan Detachment System (Burchfield et al., 1992), separates the Kinnaur Kailash Granite from high-grade paragneiss with migmatites below. About 600 m east of the confluence with the Sutlej River the Baspa transects the Karcham Normal Fault, which is localized within the Main Central Thrust Zone and finally the easternmost part of Proterozoic granitic gneiss of the Larji–Kullu–Rampur Window (Bhargava and Bassi, 1998; Srikantia and Bhargava, 1998; Hager, 2003; Vannay et al., 2004).

3. Hydrological characterization of the Baspa River

3.1. Catchment and hydrology

Based on SRTM digital elevation data the catchment area of the whole Baspa Valley is 1116 km^2 (Fig. 2). The highest point is at c. 6400 m above sea level (a.s.l.) close to Rangrik Rang and the lowest point at the confluence with the Sutlej River at 1770 m a.s.l. (Sangewar et al., 2001; Kumar and Gupta, 2001). The present tree line is situated around 3800–3900 m a.s.l. (Ranhotra and Bhattacharyya, 2010) and generally North-facing slopes show much denser forest cover than South-facing slopes.

At Chitkul (3841 m a.s.l.) 380 mm annual mean snowfall was observed between 1976 and 1990. According to Sangewar et al. (2001) the Baspa valley contains glaciers with an extent of 224 km^2 equivalent to 22% of the total catchment, which is a very

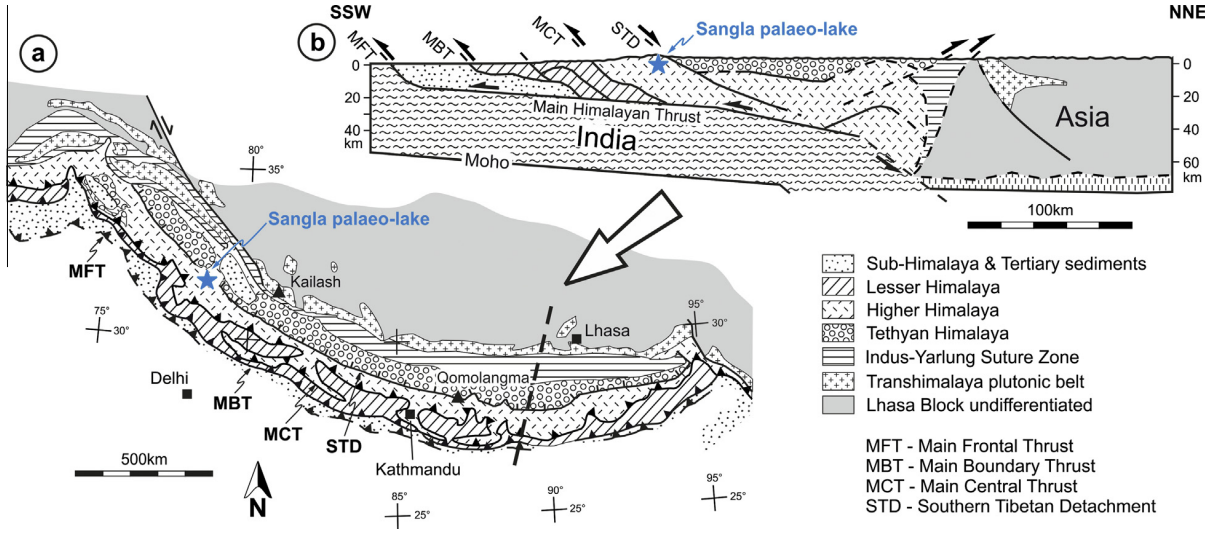

Fig. 1. (a) Tectonic map of the Himalayan orogen. Simplified after Hodges (2000). (b) Cross-section of the Himalaya interpreted from seismic data (Hauck et al., 1998). The location of Sangla palaeo-lake is indicated by a blue asterix. (For interpretation of the references to colour in this figure legend, the reader is referred to the web version of this article.)

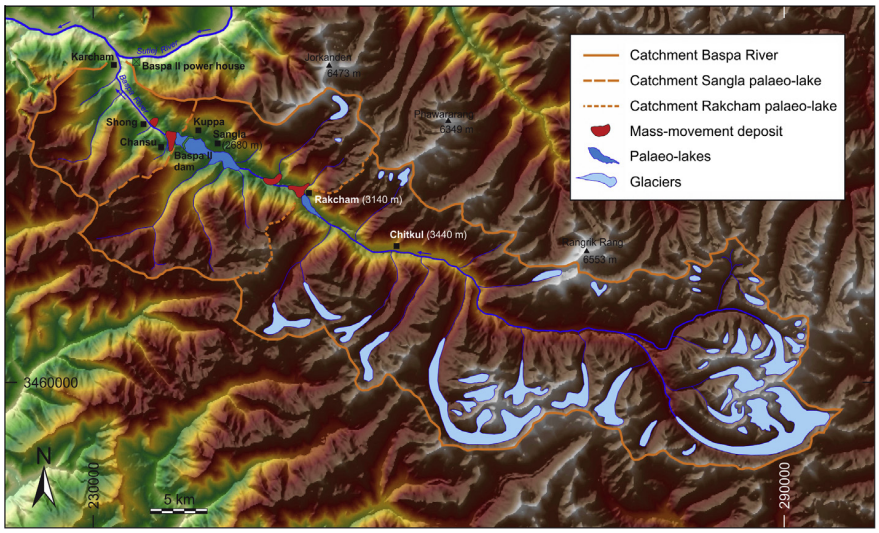

Fig. 2. Topography of the Baspa River catchment (1116 km^2) showing the mass-movements and the location of the two mass-movement dammed palaeo-lakes. Rivers and glaciers are drawn only inside the catchment. The catchments of the 3.9 km^2 Sangla palaeo-lake is 1005 km^2, while the catchment of Rakcham palaeo-lake is 764 km^2. The location of the Baspa II hydroelectric facility is indicated. Koordinates in UTM 44N.

high percentage compared to other tributaries of the Sutlej (Sangewar and Shukla, 2001). According to Sangewar and Shukla (2001) the Baspa glacier with a length of 18 km and a surface of c. 37 km^2 is the largest glacier in the Beas and Sutlej valleys of Himachal Pradesh. The comparison of the glacial extent in 1962 and 2001 shows a loss of 19% area and 23% in glacial volume (Kulkarni, 2007). At present, the equilibrium line altitude (ELA), which is the elevation of zero net snow mass balance, ranges around 5300 m a.s.l. in the Baspa catchment (Kulkarni et al., 2004).

The longitudinal profile of the Baspa River is generally convex towards the Sutlej confluence, with convex knick-points related to mass-movement deposits (Fig. 3). A pronounced change from lower gradients (0.0164 m/m^{-1}) to higher gradients (0.0326) c. 20 km east of Chitkul (Fig. 2) coincides with the lithological boundary between late Precambrian meta sediments of the Haimanta Group (Draganits, 2000; Draganits et al., 2008) in the East and Kinnaur Kailash Granite in the west (Bhargava and Bassi, 1998). In the river section directly at the palaeo-lake forming rock-avalanche at Kuppa (Fig. 2) the river gradients rises to c. 0.103.

The major part of the catchment is located above 3600 m a.s.l. (Fig. 2) and therefore the Baspa River is dominantly a glacial river regime with low discharge during winter and highest discharges during June to August, fed by melting of glacier ice and monsoonal rain (Singh et al., 2001; Wulf et al., 2012). Most of the precipitation in the catchment occurs as snow, which contributes to glacier formation, and consequently to the river flow during the period April to October. Most of the annual run off the Baspa River is derived from glacier and snowmelt. The project design 100yrs-flood is 1150 m^3 s^{-1} (JHPL, 2004).

Based on data from the weather stations at Sangla, Rakcham and Chitkul, Wulf et al. (2010) calculate 310 mm average summer precipitation and 370 mm average winter precipitation. Annual average discharge of the Baspa River between 1970 and 1990 ranged from 31 to 62 m^3 s^{-1} (Kulkarni and Alex, 2003).

3.2. Present day sediment load of the Baspa River

The amount, grain size, grain shape and mineralogical composition of the fluvial sediments are important parameters concerning the abrasion of hydroelectric installations. The measurement of the bedload of a river is quite elaborate (e.g. Emmett, 2010), therefore commonly the suspended and dissolved loads are measured.

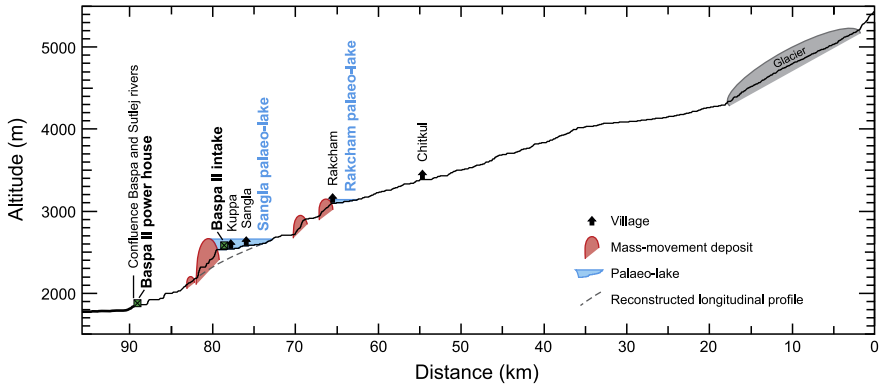

Fig. 3. Modern river profile of the Baspa River based on SRTM elevation data (Jarvis et al., 2008). Locations of relict mass-movements form clearly visible convexities, while the palaeo-lakes still show reduced river gradients. The Sangla palaeo-lake had a reconstructed maximum lake level around 2660 m a.s.l. The barrage of Baspa II hydroelectric power plant is located at 2525 m a.s.l. The maximum lake level of Rakcham palaeo-lake was around 3130 m a.s.l. The river profile before the mass-movement at the intake of Baspa II is shown by a dashed line. Original depth of the palaeo-lakes extended below the present day river profile. The location of the power house of Baspa II is projected into the section.

Bedload-to-suspended load ratio is commonly estimated at <1:10, but may reach even 1:2 in some instances (Pratt-Sitaula et al., 2007). The suspended load of the Baspa River is highest from June to August. During July the suspended load is 32.23–78.86 g per 1000 litres of river water (Singh et al., 2001). However, episodic heavy rains lasting for a few days during June to August increase the suspended load considerable. In a five years suspended load record, eight peak events with suspended load >2 g l^{-1} accounted for 62% of the total 5-years suspended sediment load (Wulf et al., 2010). Concerning grain sizes, the suspended load in upper reaches of the Baspa sums up to 4.1% fine sand, 84.8% silt, 11.3% clay, while in lower reaches the suspended load has hardly any sand and 51.0% silt with 49.0% clay (Singh et al., 2001). Clay fraction is dominated by illite and chlorite. Chemical index of alteration (CIA) of suspended sediments has an average value of 47.7 indicating negligible chemical weathering (Singh et al., 2001).

Sedimentological analysis of two samples of Baspa river sediments (fractions: <0.045 mm, 0.045–0.212 mm, >0.212 mm) shows a composition of the major minerals quartz (73.9–80.9%), biotite (10.3–15.6%) and muscovite (2.9–5.1%). The accessory minerals include feldspar (orthoclase), pyroxene (hypersthene, augite), hornblende, garnet, iron oxides and clay minerals. About 78% of the grains are sub-rounded to rounded (Baspa II, 2004).

4. Rock-avalanche dammed palaeo-lake at the site of Baspa II

4.1. Characterization of the sediments

The sedimentological properties of the lake fill including thickness of lamination, grain-size, mineralogical composition and depositional environment are a prerequisite for their comparison with modern river load sediments and catchment erosion rates. Sediments of the palaeo-lake have been deposited upstream of the rock-avalanche dam at the bridge to Chansu (Fig. 4). In general, the lake deposits are virtually free of carbonates (Fig. 7) and uncemented. The lacustrine sediments and associated alluvial fan deposits are best exposed along the road on the northern side of the Baspa River between the bridge to Chansu and Sangla (Fig. 4). Alluvial fan deposits are also very well exposed in small ravines within Sangla village (Fig. 6f). In total 8 lithological sections have been measured giving insights into proximal to distal parts of the palaeo-lake (Figs. 4–6). About 94 m of lake sediments are exposed (Fig. 5) and c. 50 m more have been documented in a drill hole at the Baspa II site (Bookhagen et al., 2005a). The sediments show general coarsening trends in upwards direction and towards the East i.e. in proximal direction. The palaeo-lake sediments consist of fine-grained bottomset and a thin gravely topset, but lack a well-developed foreset. Deformation structures comprising deformation bands as well as various types of soft sediment deformation are common (Draganits et al., 2014). Virtually no trace fossils like those in Lake Lamayuru in Ladakh (Shukla et al., 2002) have been noticed in any of the facies association.

4.1.1. Facies association A

Facies association A is characterized by grey to pale brown horizontally laminated clay-silt-fine sand; coarser laminae are preferable stained by orange-coloured Fe-hydroxides. Thickness of laminae is around 1 cm or less and they usually show pronounced normal grading. Grain size becomes smaller towards lower parts of the lake fill and towards the west. Therefore sand dominates locations 4 and 5, while the clay and silt component of the sediment increases at locations 6–8 towards the bridge to Chansu (Figs. 4–6). There a few tree leaves and charcoal have been found which were used for radiocarbon dating (Fig. 5, Table 1). Facies association A has been found from the road cut near the bridge to Chansu (2566 m a.s.l.) up to the gravel layer of facies association D (see below) at c. 2660 m a.s.l. (Fig. 5). NE of Chansu village this facies association has been deposited directly on top of the rock avalanche dam (Fig. 6a). These observations indicate an exposed thickness of 94 m of these sediments (Fig. 5), which have been deposited within c. 2400 years (radiocarbon ages in Table 1). Considering the average thickness of the laminae < 1 cm (Fig. 6b) it is obvious, that they cannot represent annual laminae (varves), instead they represent couplets that statistically have been deposited more than one time a year. This fact is supported by the modern river gauge data by Wulf et al. (2012) which indicate that in the period of observation all peak suspended sediment load events are related to heavy monsoonal rains. This facies association is interpreted as distal lacustrine sediments representing the bottomset of the lake fill. Due to the fine grain-sizes compared to other facies associations, soft sediment deformation structures in these sediments comprise normal and reverse faults, folds, overturned laminae and completely fluidized layers (Draganits et al., 2014).

4.1.2. Facies association B

This facies association comprises greyish to pale brown, mm to cm-thick, middle sand-sized sand layers. They are horizontally laminated and normally graded (Draganits et al., 2014), or commonly also show ripple cross-stratification (Fig. 6d) and climbing ripples (Fig. 6d). In some cases they are intercalated with mm- to few cm-thick clayey to silty layers. Sandy laminae are preferable stained by orange-coloured Fe-hydroxides. In areas close to alluvial fans, some cm-thick layers of greyish coarse sand to fine gravel with sub-angular clasts from the Kinnaur Kailash Granite are interbedded. Outsized clasts in these layers are <2 cm; some charcoal fragments are also found. Facies association B is interpreted as marginal lacustrine depositional environment with higher flow velocities and high deposition rates with episodic influence by distal parts of alluvial fans. Deformation structures in this facies association generally comprise conjugate normal faults (Draganits et al., 2014).

4.1.3. Facies association C

These sediments comprise sub-horizontally bedded, greyish to pale brown, 5–25 cm thick, massive, sandy, fine-grained gravel beds intercalated with a few centimetres thin, horizontally laminated or rippled fine-sand layers (Draganits et al., 2014). Channels with poorly sorted gravel are common (Fig. 6e). In areas proximal to alluvial fans the gravel beds become thicker and coarser grained up to boulder size (Fig. 6f). Generally, coarse sand and gravel grains are sub-angular and lithologically virtually comprise only fragments of Kinnaur Kailash granite, the dominant lithology in the catchment of the alluvial fan. Facies association C is found in outcrops at the rim of the alluvial fan where Sangla is built on top and is interpreted as distal part of an alluvial fan deposited in a marginal alluvial/lacustrine environment. Fig. 6f shows sandy lacustrine sediments in the lower part followed by prograding, partly wedge-shaped alluvial fan layers interbedded with thin lacustrine beds. Deformation structures in this facies association generally consist of conjugate normal faults (Draganits et al., 2014).

4.1.4. Facies association D

These deposits consists of well-rounded, poorly sorted sandy gravel with grain sizes <25 cm. The gravel is only found on top of the lacustrine sediments at locations 3 and 5b as well as NW of Kuppa (Figs. 4, 5, and 6c), where it developed a <2 m thick layer (Fig. 6c). Pebbles comprise several different lithologies including granite, grey sandstone and purple quartzite typical for Precambrian to early Palaeozoic formations (Bhargava and Bassi, 1998;

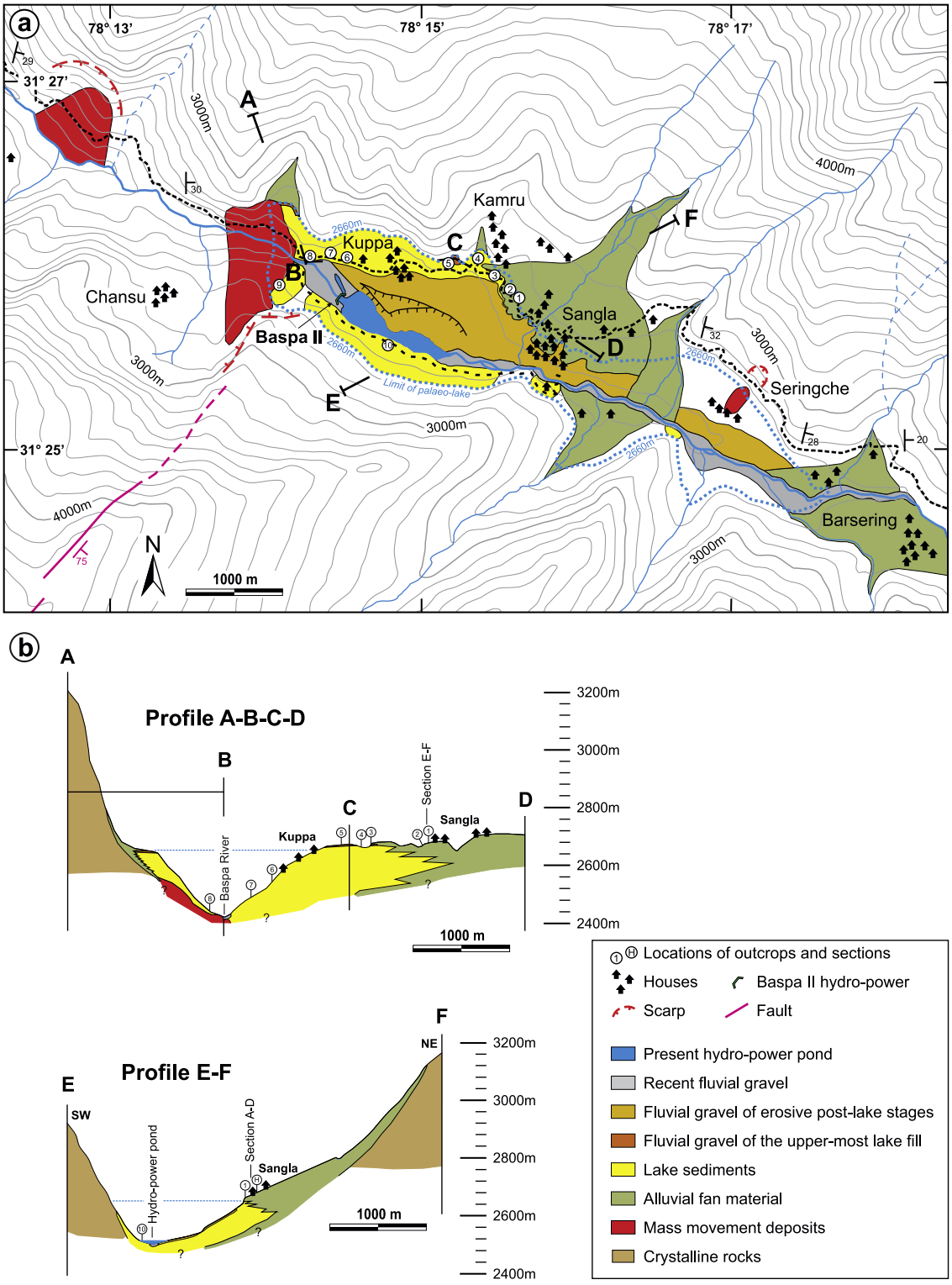

Fig. 4. (a) Geological map of the Sangla palaeo-lake lake showing the distribution of lake sediments, mass-movements and alluvial fans. The former extent of the palaeo-lake is indicated by a dashed blue line at 2660 m a.s.l. Numbers indicate locations of described outcrops and sections. Contour lines with 100 m intervals have been drawn from SRTM 4.0 elevation data. Pre-Quarternary lithologies have been kept white to improve the clarity of the figure. Baspa II is located in the palaeo-lake. Coordinates are latitude and longitude, WGS84. (b) Geological sections of the palaeo-lake. Location of the sections is indicated in Fig. a.

Draganits, 2000). Facies association D is interpreted as fluvial gravel of the Baspa River, which was deposited when the whole Sangla palaeo-lake had been completely filled up with sediment, just before head wards erosion initiated. No lake sediments have been observed above the gravel layer, which therefore represents the topset of the lake fill.

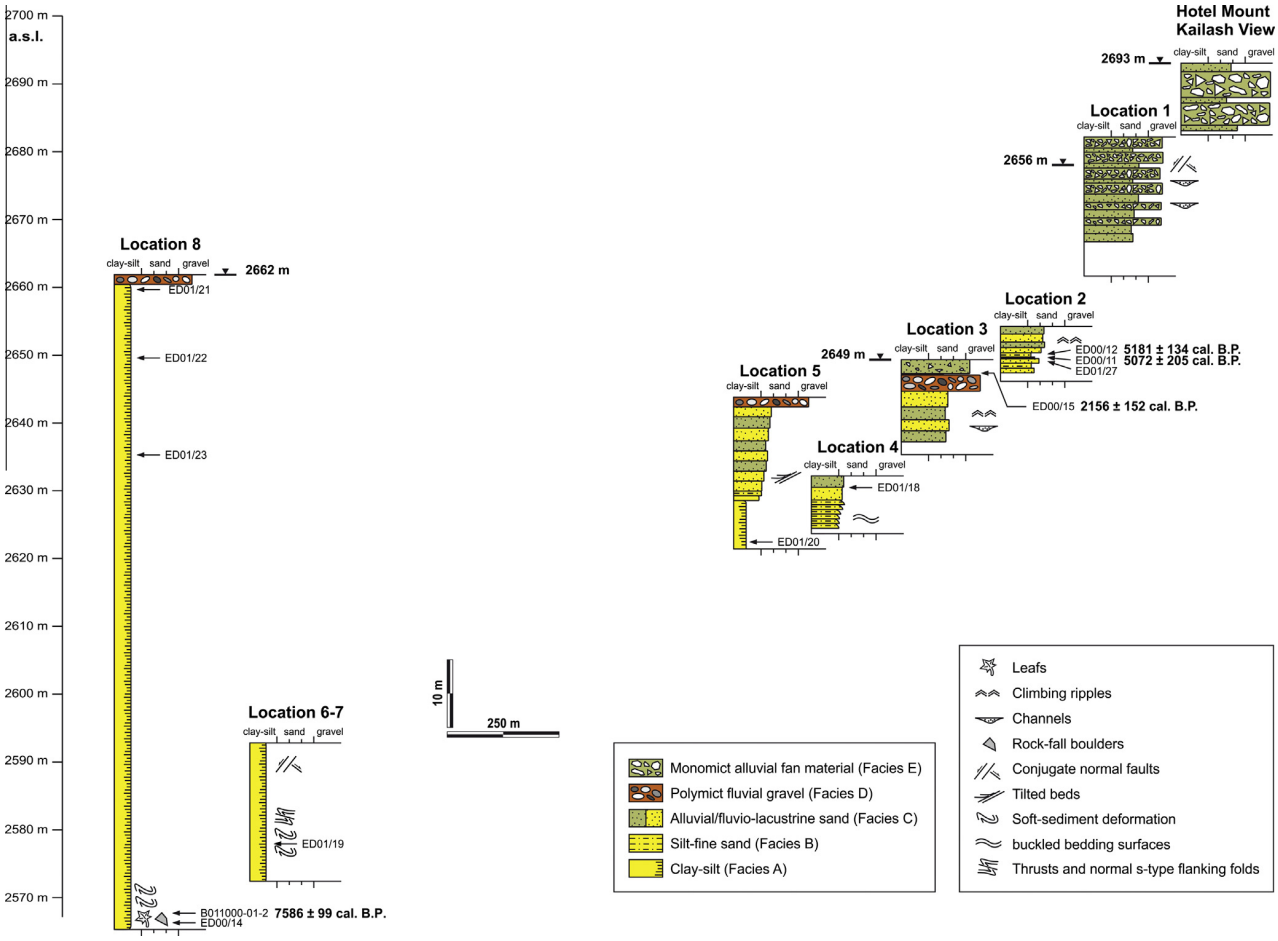

Fig. 5. Lithostratigraphic sections of Sangla palaeo-lake showing laminated lake mud and silt (bottomset), capped by fluvial gravel (topset) and the intercalation of lake sediments with alluvial layers at the lake boundaries. The location of the lithostratigraphic sections is indicated in Fig. 4a and b and broadly follow in W–E direction the road from the hydro-power installation to Sangla village. The horizontal distances between the outcrop locations are broadly at scale. The locations of sediment samples are indicated besides the sections. Radiocarbon ages with 2σ confidence intervals.

4.1.5. Facies association E

These sediments are dominated by <2 m thick, inclined beds comprising unsorted, chaotic, sub-angular gravel to boulder sized sediments. Clasts are monomict and virtually comprise Kinnaur Kailash granite (Fig. 6g). Layers of incipient soil formation may occur (Fig. 6g). Facies association E is interpreted as alluvial fan deposits formed by alluvial processes and debris flows.

4.1.6. Facies association F

Facies association F is a ridge-shaped deposit at the bridge to Chansu, which is characterized by light grey, completely chaotic, unsorted sediment with angular blocks of high-grade gneiss up to 26 m in size (Fig. 6a). The sediment shows a broad range of grain sizes with finest grain sizes comprising dominantly sand and silt with hardly any clay. This facies association is interpreted as rock avalanche deposit that dammed the Sangla palaeo-lake.

4.2. Mineralogical characterization of the palaeo-lake sediments

Nine fine-grained lake sediments from various levels of Sangla palaeo-lake were analysed by X-ray diffraction (Philips diffractometer PW 3710, Cu Kα radiation, 45 kV, 35 mA) to compare their mineralogical composition with those from the modern river load (Singh et al., 2001). All samples are very similar and are dominated by quartz, muscovite, chlorite and feldspar (Fig. 7). Sample ED01/27 additionally contains amphibol (Amph.) and talc (Tc). Furthermore, the <2 μm fraction of two samples (ED00/14, ED00/15); Fig. 5) from the lowest part of the lake and just above the topset were analysed. Fig. 8 shows the X-ray diffraction patterns of the oriented, ethylene glycol (EG) solvated <2 μm fractions of these two samples. Their mineralogical compositions are quite similar, they consist of chlorite, muscovite, quartz, K-feldspar and plagioclase; only the proportions of chlorite and muscovite show slight differences. Semi-quantitative estimates were made following the method of Schultz (1964).

Sample ED00/15 (just above the palaeo-lake topset at location 3) contains 19% quartz, 5% K-feldspar, 9% plagioclase, 64% muscovite, 3% chlorite. Sample ED00/14 (lowest exposed part of the lake at location 8) contains 15% quartz, 3% K-feldspar, 10% plagioclase, 56% muscovite, 16% chlorite. The uniformity in the mineralogical composition shows that the sediments were derived from the same source area with quite short distance of transport. The virtual lack of clay minerals indicates neglectable chemical weathering in the catchment.

4.3. Extent and volume of the rock avalanche dammed palaeo-lakes

4.3.1. Extent and volume of Sangla palaeo-lake

The reconstruction of the palaeo-lake in Fig. 9 is based on investigation of lake sediments in the field supported by SRTM 4.0 elevation data (Jarvis et al., 2008). These elevation data have significantly lower resolution (90 × 90 m) than airborne laser

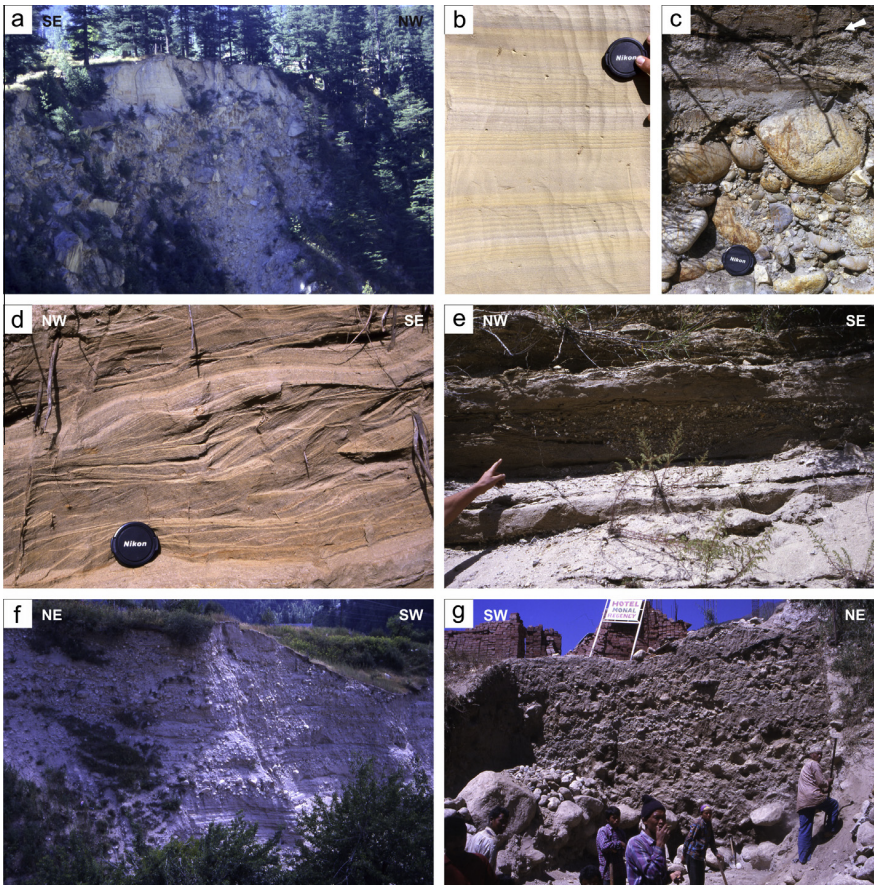

Fig. 6. Investigated Holocene sediments. For location see Fig. 4a. (a) Coarse grained rock avalanche deposits from the rock-avalanche dam at location 9 are covered by a few meters of laminated lake mud. (b) Well developed lamination of fine sand and mud at location 4; the lamination does not show annual cyclicity. (c) Polymict fluvial gravel of the topset at location 3; arrow points to black charcoal layer above where sample ED00/15 has been taken. (d) Lacustrine sands with ripple cross bedding and climbing ripples at location 5. (e) Lake sand intercalated with coarser, angular, monomict alluvial fan sediment at location 1. Note the channel structure. (f) Deeply eroded gully in the centre of Sangla village showing fine grained, laminated lake sediment at the base and upwards gradually interfingering with coarse alluvial fan deposits, which finally replace them completely. (g) Coarse, monomict alluvial fan sediment in Sangla.

scanning data (1 × 1 m) used by Mackey et al. (2011) to investigate the palaeo-lake of the Eel River in California. The highest observed lake sediments are situated between 2642 m and 2660 m a.s.l. (Fig. 5) and therefore the extent of the palaeo-lake is based on the 2660 m a.s.l. contour line of the present topography calculated from SRTM data 4.0. Based on the outcrop observation of lake sediments and the present topography the palaeo-lake is reconstructed to a length of 6.1 km and a maximum width of c. 1.4 km. The surface of palaeo-lake is calculated to c. 3.9 km^2. Due to slope wash deposits and alluvial fan sediments on top of the palaeo-lake, this size is interpreted as minimum value. Especially the comparable flat surface of the large alluvial fan where Sangla has been built on top probably covers former extensions towards the north-east of the palaeo-lake (Fig. 4).

The reconstruction of the former lake volume is difficult, because the reconstruction of the valley shape prior to the palaeo-lake and possible existing fluvial and alluvial sediments contain many uncertainties. We have used following observations of the lake extent and cross-section considerations for the estimation of the palaeo-lake volume:(1) estimated depth of c. 260 m constrained by: (a) the location of the uppermost lake sediments are found at 2645–2660 m a.s.l. at the northern valley side close to the mass-movement dam (Figs. 4 and 5); (b) The lowest exposed lake sediments are found at the road close to the bridge to Chansu at 2566 m a.s.l.; (c) at least 50 m lake sediments in a drill hole in the area of the barrage (located around 2525 m a.s.l.) mentioned by Singh and Jain (2001); (d) reconstructed depth (c. 2400 m a.s.l.) of the valley at the Baspa II dam location prior to the rock avalanche, based on the reconstruction of the longitudinal section of the Baspa River (Fig. 3) indicating a maximum depth of about 260 m for the palaeo-lake. (2) A maximum palaeo-lake width of 1400 m at its downstream part and a lake shape gradually tapering upstream (Fig. 4). (3) A total length of the palaeo-lake of 6100 m, reconstructed by the field observation of lake sediments and reconstruction of the lake extend based on the 2660 m a.s.l. contour line (Figs. 4 and 9).

Based on these observations and presuming an overall V-shaped outline of the valley prior to the mass-movement, the volume of the lake was calculated as an irregular tetrahedron using

$$V = \frac{1}{6} \cdot w \cdot \mathrm{l} \cdot \mathrm{d} \quad (1)$$

w is the maximum palaeo-lake width, l is palaeo-lake length, and d is maximum depth.

Using the reconstructed total depth estimation results in a volume of c. 3.7×10^8 m^3, *versus* 1.15×10^9 m^3 calculated by Bookhagen et al. (2005a, p. 151) who have assumed that the valley prior to landsliding and paleolake existence has been empty as the landslides abut on bedrock in many places. Using a parabola-shaped valley for the calculation of the whole palaeo-lake volume,

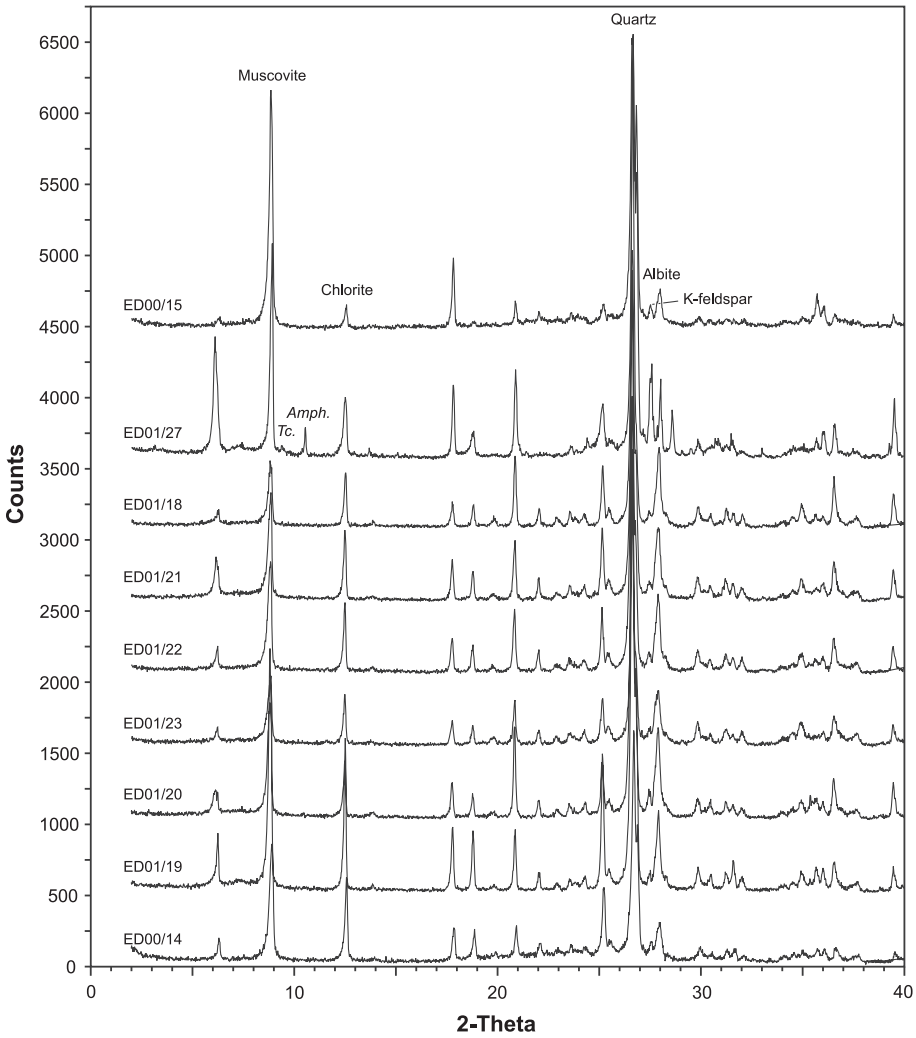

Fig. 7. X-ray diffraction patterns of lacustrine sediment samples from various levels of Sangla. Diffraction patterns are organized from bottom to top in stratigraphic order (see Figs. 4 and 5 for their location). All samples show very similar mineralogical composition dominated by quartz, muscovite, chlorite and feldspar. Sample ED01/27 additionally contains amphibol (Amph.) and talc (Tc).

Table 1
Radiocarbon ages from Sangla palaeo-lake. All samples measured by Vienna Environmental Research Accelerator (VERA), except B011000-01-2, which has been analysed by Leibniz Labor für Altersbestimmung und Isotopenforschung, Christian-Albrechts-Universität Kiel (Bookhagen et al., 2005a).

Sample	Laboratory number	$d^{13}C^{*}$ (‰)	^{14}C-age* (BP)	Calibrated age**
ED00/15[a]	VERA-1669	−24.3 ± 1.0	2150 ± 40	2156 ± 152 cal yr BP
ED00/11[b]	VERA-1667	−21.9 ± 0.9	4420 ± 40	5072 ± 205 cal yr BP
SED00/12[c]	VERA-1668	−20.6 ± 0.9	4535 ± 40	5181 ± 134 cal yr BP
B011000-01-2[d]	KIA16074	−25.8 ± 0.1	6730 ± 60	7586 ± 99 cal yr BP

[a] Charcoal layer (Fig. 7c).
[b] Charcoal layer (Fig. 10).
[c] Charcoal (Fig. 10).
[d] Charcoal (Bookhagen et al., 2005a).
* 1σ confidence interval.
** Calibrated with OxCal v4.1.7 (Bronk Ramsey, 2010), 2σ confidence interval.

would increase the volume by one third. Estimating the lake volume just for the thickness of the exposed lacustrine sediments (94 m) results to some 2.9×10^8 m^3, which means c. 77% of the total lake volume. For the upper part of the palaeo-lake the difference between the different shapes (V-shape, parabola, hyperbola) becomes less important.

4.3.2. Extend and volume of Rakcham palaeo-lake

The size of Rakcham palaeo-lake is much smaller than the one at Sangla. Similar to Sangla palaeo-lake, thin fluvial gravel on top indicates that also this palaeo-lake had been completely filled with sediments, before the dam was eroded. The lake sediments have been traced up to c. 3130 m a.s.l. and the former lake covered

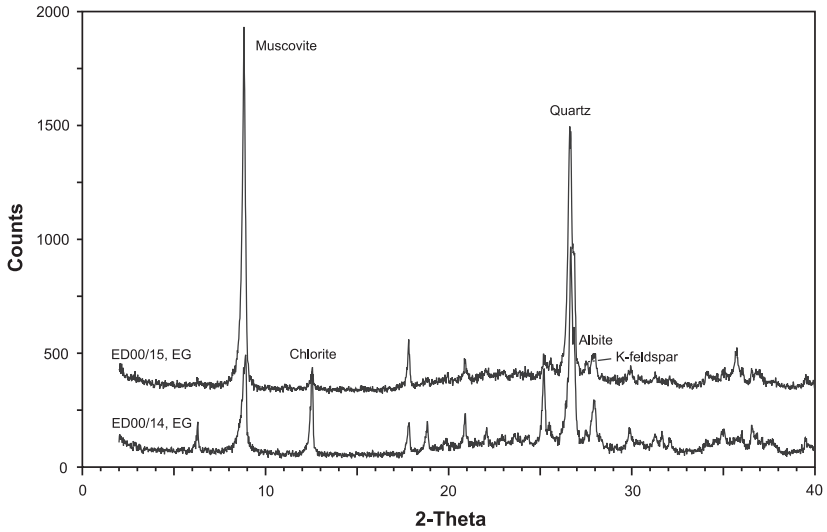

Fig. 8. X-ray diffraction patterns of oriented, ethylene glycol solvated <2 μm fractions of two lake sediment samples (ED00/14, ED00/15; Fig. 5). Their mineralogical compositions are quite similar, consisting of chlorite, muscovite, quartz, K-feldspar and plagioclase; only the proportions of chlorite and muscovite show slight differences. Patterns are very similar with the untreated samples (Fig. 7) because of the lack of expandable minerals.

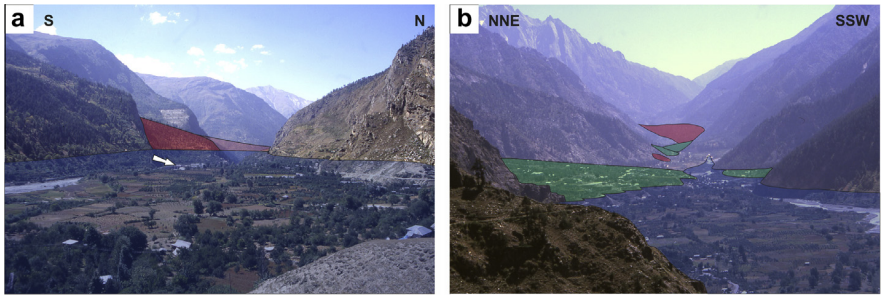

Fig. 9. Reconstruction of the Sangla palaeo-lake. (a) View towards the west to the rock-avalanche deposits that dammed the Sangla palaeo-lake. Location of Baspa II, c. 130 m below the maximum lake surface of Sangla palaeo-lake, is indicated by a white arrow. (b) View towards east-south-east. Note alluvial fans in the middle ground and other rock-avalanche deposits in the background.

1.2 km^2. Using the same formula for the volume of an irregular tetrahedron and based on a maximal width of 630 m close to the rock avalanche dam, a length of c. 3000 m as well as estimated depth of 40 m, the volume of Rakcham palaeo-lake is estimated to some 0.13×10^8 m^3.

4.4. Age of the palaeo-lake sediments

The age of the lacustrine sediments of Sangla palaeo-lake have been assessed by radiocarbon dating of four samples of organic material (Figs. 6c, and 10; Table 1) applying standard cleaning and analytical procedures.

Tree leaves and charcoal in lacustrine mud from the lowest exposed lake sediments (location 8) at the bridge to Chansu have an age of 7586 ± 99 cal yr BP (Bookhagen et al., 2005a), which also represents the minimum age for the rock-avalanche dam. A charcoal layer (5072 ± 205 cal yr BP) and a piece of charcoal (5181 ± 134 cal yr BP) from the uppermost lake sediments at location 2 (Figs. 4 and 5) are interpreted to represent the final stage of lake filling. The fluvial gravel covers the uppermost palaeo-lake sediments and represents a striking marker bed that has been recorded at 2660 m a.s.l. (location 8), 2643 m a.s.l. (location 5) and 2645 m a.s.l. (location 3) (Fig. 8). No lake sediments have been observed above this gravel layer and the present occurrence at different altitudes is explained by deformation after its deposition (Draganits et al., 2014).

These three radiocarbon ages indicate duration of 2495 ± 297 years for the lake silting of the exposed c. 94 m of the lake fill. This number represents the minimum duration for the filling of the whole lake, as the entire unexposed lake sediments below have not been dated.

The youngest measured radiocarbon age of 2156 ± 152 cal yr BP is from a charcoal layer at location 3, sandwiched between the fluvial gravel of the topset below and alluvial fan sediments above (Figs. 4, 5, 6c). Therefore this layer was deposited after the lake had been filled completely. This charcoal layer is located close to the modern soil and therefore also contamination cannot be excluded.

4.5. Vegetation and palynomorph flora

Today the vegetation cover of the investigated area is generally a conifer mixed broad-leaved forest typical for this height zonation (Polunin et al., 1999; Shrestha, 1989), comprising the conifers *Pinus wallichiana* and *Cedrus deodar* and the broad leaved angiosperm such as various *Quercus* species, *Ulmus wallichiana*, *Juglans regia, Acer caesium* and *Betula utilis* etc. Betula reaches up to the upper tree limit (up to 3900 m a.s.l.) together with intermingled *Juniperus* sp., above this height alpine steppe dominates (grasses and herbs)

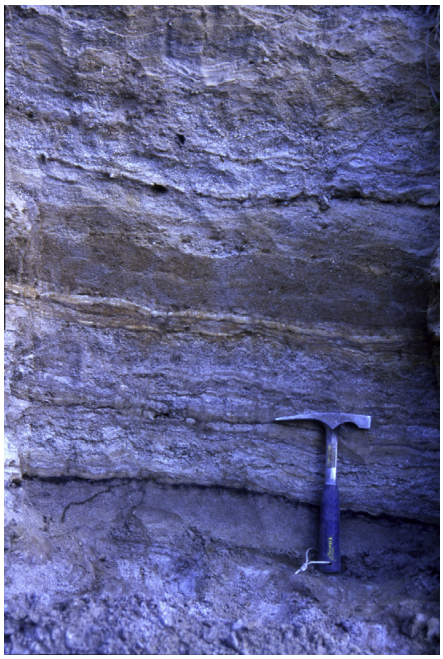

Fig. 10. Two thin charcoal layer and pieces of charcoal in silty/sandy lacustrine layers intercalating with sandy to fine gravelly alluvial fan layers in the uppermost part of the lake at location 2. Sample ED00/11 from the lower charcoal layer shows a radiocarbon age of 5072 ± 205 cal yr BP and the large charcoal fragment ED00/12 from the upper charcoal layer an age of 5181 ± 134 cal yr BP (Table 1).

(Stainton, 1972; Polunin et al., 1999; Ranhotra and Bhattacharyya, 2010).

In total ten fine-grained lake samples have been analysed for diatoms, but none have been found (pers. comm. Ingrid Jüttner). Eleven fine-grained samples of fine-grained lake sediments have been analysed palynologically, but only two of them contained pollen (Fig. 11). These two samples display very distinct assemblages (Fig. 12).

The lower sample ED00/14 originates from the deepest exposed part of the palaeo-lake at location 8 (2566 m a.s.l., 7586 ± 99 cal yr BP; Bookhagen et al., 2005a) (Figs. 4 and 5). This sample is characterized by the abundance and diversity of angiosperm trees and shrubs, particularly evergreen Fagaceae, and ferns and fern allies, all of which indicate moist and temperate conditions (Figs. 11a–j, and 12). The forest types reflected in this assemblage can be ascribed to a zonal "upper temperate mixed evergreen broad leaved forest" (palynomorph taxa: *Acer, Alnus, Betula, Castanopsis* spp., *Carpinus, Fraxinus, Juglans, Quercus* spp. and *Ulmus*, etc.) that was intermixed in the higher regions with a "temperate conifer forest" (palynomorph taxa: *Abies, Cedrus, Picea, Pinus* spp. – mostly Haploxylon-type) and partly reflects the living vegetation at the investigated site. Both forest types occur today between c.1500 and 3300 m a.s.l. and mainly inhabit the moist north and west facing slopes of the western Himalaya range (Stainton, 1972; Polunin et al., 1999; Shrestha, 1989). Only taxa adapted to relatively dry conditions (*Quercus semecarpifolia*, *Juniperus* sp. and *Pinus roxburghii*) grow on south facing slopes (Stainton, 1972). The subfossil "upper temperate mixed evergreen broad leaved forest" assemblage is characterized by a rich understorey of shrubs (palynomorph taxa: *Ilex, Hippophae, Myrica, Rhamnus, Rosaceae, Stellera, Rhus*). The diverse fern flora (Aspleniaceae, Dryopteridaceae, Polypodiaceae, Pteridaceae, etc.) and the humidity loving (azonal) shrubs such as *Alnus* are thought to have grown in damp gullies and at the bottom of the valley, beside streams or standing water bodies.

The upper sample ED00/15 derives from a charcoal horizon directly above the polymict fluvial gravels that cap the lake deposits (2648 m a.s.l., 2156 ± 152 cal yr BP) (Figs. 4, 5, and 6c). This sample apparently reflects a drier environment or an alpine steppe vegetation (generally above 4000 m a.s.l.), with abundant grassy and herbaceous vegetation (two types of Poaceae, *Artemisia*, Asteraceae, Caryophyllaceae, Chenopodiaceae, *Impatiens*, Lamiaceae), surrounding azonal water bodies (Table 2, Figs. 11k–o and 12). The water bodies, which were fringed by a few *Typha* and Cyperaceae stands and a few angiosperm shrubs and trees (e.g. *Alnus, Myricaria*), was inhabited by freshwater algae (several Zygnemataceae taxa and *Botryococcus*) the latter providing evidence of more oligotrophic conditions. The input of temperate coniferous taxa *Abies* and *Cedrus,* is much lower except that of *Picea* (mostly on northfacing slopes) and *Pinus* (mostly haploxylon type).

5. Discussion

5.1. Palaeo-climate

Plentiful studies have been carried out on present day glacial inventory and glacial retreat in the Baspa Valley (Sangewar and Shukla, 2001; Sangewar et al., 2001; Kulkarni et al., 2004; Kulkarni, 2007; Ranhotra and Bhattacharyya, 2010; Bali et al., 2013), but virtually no investigation of the early Holocene or late Pleistocene glaciation exist in this area, where high erosion rates efficiently remove deposits and landforms of older glaciations. The lowest clearly recognizable moraines from a left hand tributary valley glacier are located around 3300 m a.s.l.

The Bhagirathi Valley is less than 20 km SE of the upper reaches of the Baspa Valley in a similar orographic position and therefore palaeo-glacial studies there (Sharma and Owen, 1996; Barnard et al., 2004) might be used as an analogue. In the Bhagirathi Valley Sharma and Owen (1996) locate the maximum extent of ice at Jhala at 2450 m a.s.l., based on a change in valley form and a sharp ridged moraine, which was dated to c. 63 kyr. In the Baspa Valley a similar change in valley form can be found at the bridge to Chansu, at the western termination of the Sangla palaeo-lake at 2560 m a.s.l. Upstream of this location the Baspa Valley is quite a broad U-shaped valley, while downstream the Baspa has cut a V-shaped valley, responsible for a spectacular road construction in this area. In the upper Tons Valley (Garhwal), to the east of the Baspa Valley, the lowest glacial moraines also have been found at c. 2500 m a.s.l. having a ^{10}Be-exposure age around 16 ka (Scherler et al., 2010).

Glacial sediments and OSL dating of late Pleistocene to Holocene sediments in Lahaul indicate that glacier advances correlate more with the availability of snow than with cold temperatures (Owen et al., 2001). In intervals of strengthened South Asian summer monsoons (e.g. Bookhagen et al., 2005b) the monsoon extends its influence further north, resulting in a positive mass-balance of snow. Data indicate that the maximum advances of glaciers in the Himalaya occurred early in the last glacial cycle, commonly during marine isotope stage (MIS) 3 c. 60–53 kyr with relatively warm climates and increased monsoon precipitation (Owen et al., 2002). During the global Last Glacial Maximum LGM (c. 24–18 ka), glacier advance in the Himalayas was restricted to less than 10 km of their present ice fronts (Owen et al., 2002). Therefore the glaciation in the Himalaya was not synchronous with oscillations in Northern Hemisphere ice-sheets (Owen, 1998; Scherler et al., 2010). The distribution of modern glaciers in the Baspa catchment shows, that the closer they are located to the Sutlej Valley, the main route for Monsoon moisture (Bookhagen et al., 2005b) the lower is the altitude of their termination (Fig. 2). These characteristics probably underline the importance of the amount of

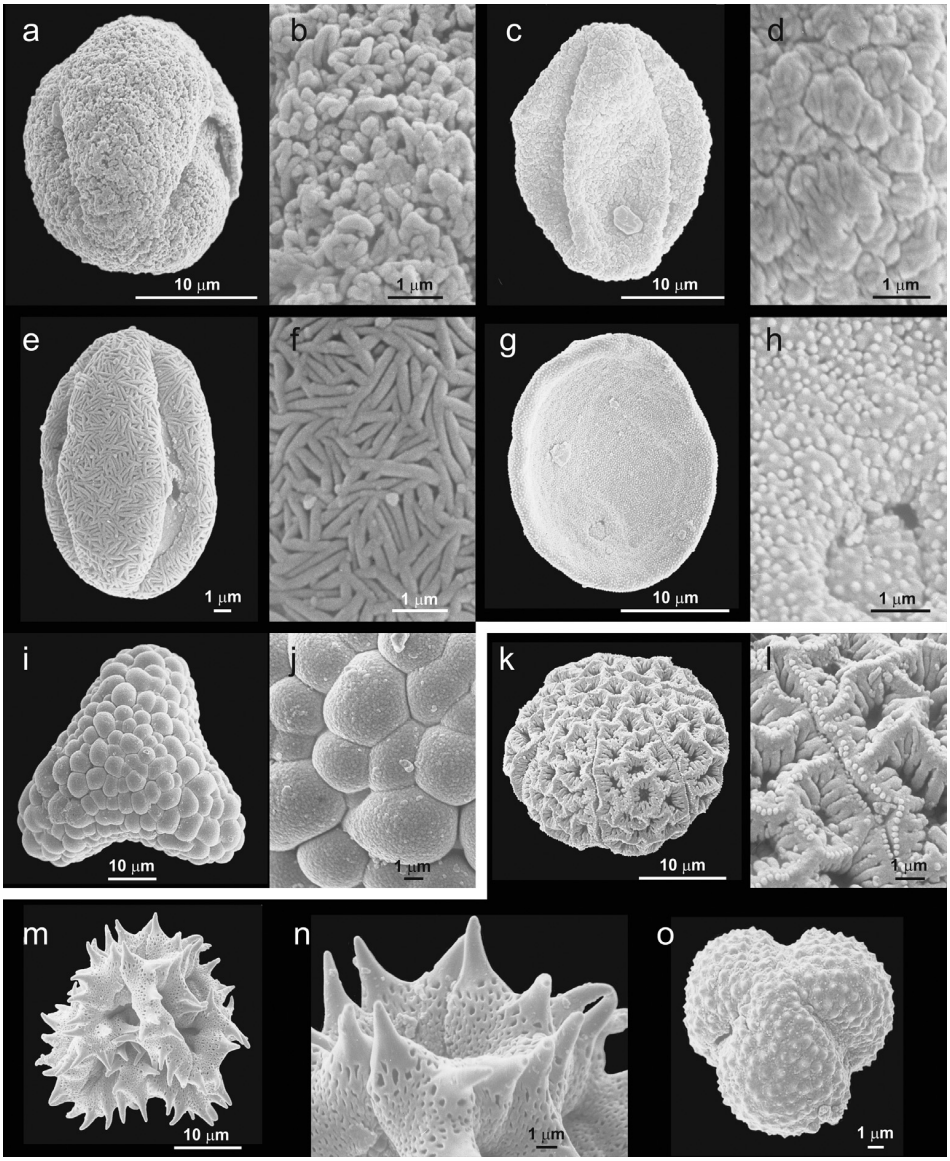

Fig. 11. SEM photos of selected pollen from samples ED00/14 (a–j) and ED00/15 (k–o). (a) *Quercus semecarpifolia*. (b) Detail of *Quercus semecarpifolia*. (c) *Quercus ?leucotrichophora*. (d) Detail of *Quercus ?leucotrichophora*. (e) *Castanopsis ?tribuloides*. (f) Detail of *Castanopsis ?tribuloides*. (g) Poaceae gen. indet. 1. (h) Detail of Poaceae gen. indet. 1. (i) Fern gen. indet. (j) Detail of fern gen. indet. (k) *Polygonum* sp. (l) Detail of *Polygonum* sp. (m) Asteraceae ("lactuceae"). (n) Detail of Asteraceae ("lactuceae"). (o) *Artemisia* sp.

precipitation for Himalayan glaciers (Owen, 1998; Owen et al., 2001).

Climate and especially the amount of precipitation and its distribution throughout the year controls river run-off – a crucial parameter for the operation of a hydroelectric installation – and last but not least an important factor for slope stability (Bull, 2009).

Precipitation in the NW Himalaya is controlled by two atmospheric circulation systems (Gadgil, 2003; Bookhagen and Burbank, 2010). During the Indian summer monsoon moisture mainly arrives from the Bay of Bengal from June to September. During December to March the Northern-Hemisphere westerlies supply moisture (Putkonen, 2004). The Himalayan topography exerts a strong control on the amount and regional distribution of the precipitation (Bookhagen et al., 2005b; Bookhagen and Burbank, 2010).

Nowadays there is quite a dense network of meteorological stations installed in the NW Himalaya (Wulf et al., 2010, 2012), but for the pre-instrumental period we depend on palaeoclimatic proxies including stable isotopes and pollen. Unfortunately, high resolution temperature and precipitation data like those by Treydte et al. (2006) on oxygen isotopes of tree rings do not exist in the NW Himalaya. Most of the papers utilize pollen data from lake sediments as climate proxies, commonly with only meagre climate and time resolution (Trivedi and Chauhan, 2009). Additionally, in several publications about lake pollen in this area it is unclear if the radiocarbon ages are calibrated or not.

The regionally closest palaeoclimatologic study is by Chakraborty et al. (2006), in a left hand tributary valley to the Baspa River some 4 km SW of Sangla, investigating 1.3 m thick lake sediments with an age range of 10450 ± 310 to 1800 ± 64 uncal yr BP. Similar to our results, the pollen between 10450 ± 310 and 4510 ± 56 uncal yr BP, are interpreted to indicate relatively warm and moist conditions with many trees. The sediments between 4510 ± 56 and 1800 ± 64 uncal yr BP were devoid of pollen, but rich

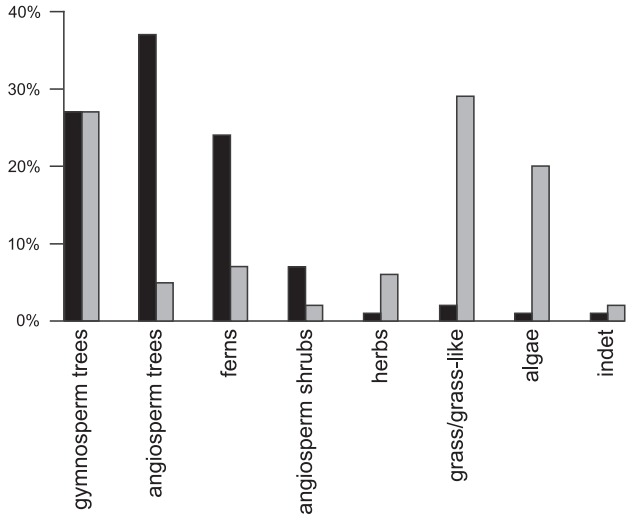

Fig. 12. Histogramm of the abundance of important pollen groups. Pollen from a clay (ED00/14) in the lowermost part of the lake, close to the dam (black column), show a relatively diverse flora (65 taxa) indicating considerable warmer and more humid climate (e.g. 25 taxa of ferns and fern allies) close to the time, when the rock-avalanche occurred, than a less diverse flora (23 taxa) in clay (ED00/15) directly above the lake sediments (gray column).

in charcoal. The sediments younger than 1800 ± 64 uncal yr BP were rich in steppe vegetation (Chakraborty et al., 2006).

The pollen samples from the base of the exposed Sangla palaeo-lake sediments near the bridge to Chansu (ED00/14; 2566 m a.s.l.) is characterized by the abundance and diversity of angiosperm trees and shrubs, particularly evergreen Fagaceae, and ferns and fern allies, all of which indicate moist and temperate conditions. These observations of relatively moist conditions fit nicely to relatively high monsoon activity modelled by Prell and Kutzbach (1987) as well as high lake levels of Tso Kar in Ladakh (Wünnemann et al., 2010) in a period, when the sediment of ED00/14 was deposited (7586 ± 99 cal yr BP; Bookhagen et al., 2005a) (Fig. 5, Table 1). The pronounced difference from the pollen sample just above the palaeo-lake (ED00/15; 2648 m a.s.l.) like the decrease in angiosperm shrubs and trees (particularly several evergreen *Quercus* and *Castanopsis* taxa, except *Quercus semecarpifolia*) can be interpreted either as a decrease in humidity on the lower valley slopes and therefore successive disappearance of the mixed forest type and encroachment of alpine steppe elements, or because of the increasing dryness, the mixed forests on the slopes were destroyed by fire and were succeeded by secondary growth (grasses and herbs). The latter is supported by the occurrence of charcoal in the palynomorph extract and slight increase of the diploxylon *Pinus* (e.g., *P. roxburghii*) which can withstand fires (Stainton, 1972).

Sedimentary clays have been used as indicators for paleoclimatic conditions, too (Chamley, 1989). The presence of only chlorite and muscovite (or illite) in the samples indicates a rather cold and dry climate with dominant physical weathering (Chamley, 1989), which is supported by an average chemical index of alteration (CIA) value of 47.7 indicating virtually no chemical weathering (Singh et al., 2001). Dominant chemical weathering (hydrolysis) would lead to the formation of mixed layer- or expandable clay minerals, which were not detected in the samples.

5.2. Denudation rates in the Baspa catchment from Sangla palaeo-lake

Upstream of Sangla palaeo-lake there exist two additional palaeo-mass-movement dams (Fig. 2) that have to be considered as possible sediment traps for the calculation of the sedimentation rates from Sangla palaeo-lake. As discussed by Draganits et al. (2014), the probable relative age succession of the rock avalanches, based on their appearance, from older to younger are: (1) Kuppa, (2) Rakcham and (3) East of Basering. Calculations based on the volume of Sangla palaeo-lake depend strongly on the age of the upstream landslide-dammed palaeo-lake at Rakcham, because if both lakes existed at the same time the Rakcham palaeo-lake would have trapped sediments of the Baspa and would thus reduce erosion rate estimates. The mass-movement east of Basering is neglected in this discussion, because it probably dammed just a small lake if ever.

No material suitable for radiocarbon dating have been found in Rakcham palaeo-lake, therefore theoretically four scenarios are possible: Rakcham palaeo-lake is (i) older, (ii) existed at the same time, (iii) overlapped partly or is (iv) younger than Sangla palaeo-lake. Assessing this question by progressive landscape evolution, Rakcham mass-movement deposit is considerable less covered by trees and soil compared to the Kuppa dam and therefore is obviously younger. Even if Rakcham palaeo-lake existed at least partly at the same time as the Sangla palaeo-lake, it represents just 3% of Sangla palaeo-lake volume (Section 4.3.2) and therefore has been neglected for the reconstruction of the palaeo-denudation rate.

We have used following figures for the calculation of the catchment erosion rates from the volume of the exposed Sangla palaeo-lake: (a) 1005 km^2 catchment area from SRTM digital elevation data (c. 90% of the whole Baspa watershed), which is slightly larger than the catchment of 968 km^2 calculated for the location of the dam of the Baspa II hydroelectric station (JHPL, 2004), which is situated some 450 m upstream of the rock avalanche dam, (b) lake volume of 2.9×10^8 m^3 of the upper 94 m thick exposed lake sediments (c. 77% of the whole lake volume, see Section 4.3.1), (c) duration of sedimentation of the exposed lake sediments of 2495 ± 297 years (Section 4.4). The dry sediment bulk density is a crucial factor for the conversion of lake sediment volume into erosion rates (Verstraeten and Poesen, 2001); unfortunately it is not always mentioned in papers dealing with erosion rates. We have estimated the dry sediment bulk density of the >5000 yr old, quite well consolidated lake deposits dominated by mud and fine sand between 1800 and 2000 kg m^{-3}. The average density of the rocks in the catchment was estimated to 2700 kg m^{-3}. Using 1800 kg m^{-3} and 2000 kg m^{-3} dry sediment bulk densities for the lake sediments result in catchment erosion rates of Sangla palaeo-lake of 0.7–0.9 and 0.8–1.0 mm yr^{-1}, respectively. These are minimum values because dissolved load was not considered. It is remarkable that these palaeo-erosion rates in the Baspa catchment are exactly in the range of modern erosion rate values (0.9–1.5 mm yr^{-1}) calculated for the three main basins of Nepal by Andermann et al. (2012).

Based on detailed measurements of the sediment load at the Baspa II site, the average present day erosion rate of the Baspa River based on suspended sediment load and bedload from 2004 to 2008 is 1.05 ± 0.8 mm yr^{-1} (see Wulf et al., 2010 for details). Bookhagen et al. (2005a) calculated 4.3 ± 0.4 mm yr^{-1} palaeo-denudation rates from the Sangla palaeo-lake sediments based on (i) 1.15×10^9 m^3 lake volume, (ii) 2370 ± 86 yr of lake existence and (iii) 115 km^2 catchment of Sangla palaeo-lake assuming the existence of upstream palaeo-lakes acting as sediment traps (Fig. 2). All these catchment denudation rates are quite small compared to the orogenic scale Plio-Quaternary erosion rates calculated from bedrock mineral cooling ages from the Himalaya indicating long-term erosion rates of 1.8–5.0 mm yr^{-1} (Whipp et al., 2007; Thiede and Ehlers, 2013). The discrepancy between the Holocene and modern rates discussed above with the long-term rates may be explained by the high erosional efficiency of glaciers, scarcity of vegetation in glacial phases and high transport

Table 2
Palynomorph flora and percentage distributions of taxa of the two samples ED14 and ED15 from the Sangla palaeolake. Modern day approximate altitudinal ranges of individual taxa are compiled from Collett (1902), and Stainton (1972).

Gymnosperms	Genus	Species/-number	ED0014	ED0015	Altitudinal range
Pinaceae	*Abies*	*pindrow*	4.3	1	2400–2700
	Cedrus	*deodara*	6.3	2.6	1800–3000
	Larix	*griffithiana*		acc.	2800–4000
	Picea	*smithiana*	3.7	4.3	2100–2700
	Pinus	*wallichiana type*	10.7	10.1	1500–3000
	Pinus	*roxburghii type*	1.4	5.6	1000–2500
Angiosperms					
Aceraceae	*Acer*		acc.		800–3000
Anacardiaceae	*Rhus*		acc.		1500–2400
Aquifoliaceae	*Ilex*	*dipyrena-like*	acc.		1500–2400
Asteraceae	"lactuceae"	2 types	acc.	acc.	
	tubuliflore type		acc.		
	Artemisia		acc.	3.7	900–3600
Balsaminaceae	*Impatiens*			acc.	1500–3600
Betulaceae	*Alnus*	?2 types	6.7	1.9	900–2700
	Betula	?2 types	4.7	1.6	1500–2700–4300
	Carpinus	*?viminea*	acc.		
Caryophyllaceae	gen. indet.		acc.	acc.	
Chenopodiaceae	*Chenopodium*		acc.	acc.	up to 3600
Convolvulaceae	gen. indet.		acc.		
Cornaceae	*Cornus*		acc.		900–2400
Cyperaceae	gen. indet.		1	acc.	
Eleagnaceae	*Hippophae*		acc.		
Ericaceae	*gen. indet.*			acc.	
Fagaceae	sensu lato	2 types	1.8		
	Castanopsis	*?tribuloides*	2.6		1000–2400
	Quercus	5 types	18.7	1.9 (2)	1500–2700
Juglandaceae	*Juglans*	*regia*	1.8		2100–3000
Lamiaceae	indet.			acc.	
Myricaceae	*Myrica*		acc.	acc.	below 1800
Oleaceae	*Fraxinus*	*floribunda*	1.6		1500–2700
Poaceae	gen. indet. 1	(20 mμ)		20	
	gen. indet. 2	(30 mμ)	1.2	8	
Polygonaceae	Polygonum			acc.	
Rhamnaceae	*Rhamnus*		1		1200–3000
	gen. indet.		acc.	acc.	
?Sapotaceae	gen. indet.		acc.		
Salicaceae	*Salix*		acc.		
Thymelaceae	*Stellera*		acc.		1800–3000
Typhaceae	*Typha*		acc.	1	
Ulmaceae	*Ulmus*	*wallichiana*	2.2	acc.	1200–2400
Urticaceae	gen. indet.		acc.		
Vitaceae	*?Leea*		acc.		below 1500
Ferns and fern allies					
Aspleniaceae	*Asplenia-type*		acc.		
Dryopteridaceae	*?Acrophorus*		acc.		
	?Dryopteris		acc.		
	?Nothoperanema		acc.		
	Polystichium		acc.		
Lycopodiaceae	*Lycopodiella*		acc.		
Ophioglossaceae	*Botrychium*		acc.		
Osmundaceae	*Osmunda*		1		
Polypodiaceae	sensu lato	2 types	18.4	5.6	
	Polypodium	2–3 types	1		
Pteridaceae	sensu lato	3 types	acc.		
	Cryptogramma		acc.		
	Pteris		acc.		
Marchantiaceae	*Riccia-like*		acc.		
Sphagnaceae	*Sphagnum*		1		
Thelypteridaceae	*Thelypteris*		acc.		
fam. indet.	*fern massula*		1		
Freshwater algae					
Zygnemataceae	gen. indet.	3 types	1	9.3	
	Spirogyra	3 types		4	
	Mougoetia	2–3 types		acc.	
	Zygnema			5.3	
Botryococcaceae	*Botryococcus*			3.2	
	indet.		1.6	2	

capacities in periods of deglaciation during the Pleistocene (Hinderer, 2001; Gabet et al., 2008).

5.3. Early indications for human presence in the Baspa Valley?

The Himalaya as well as the Tibetan Plateau are extreme environments. Available archaeological evidence in this area is very rare and consequently timing, motivation and directions of earliest colonization are still poorly understood (Brantingham et al., 2007; Rhode et al., 2007; Meyer et al., 2009; Kaiser et al., 2009).

The Baspa catchment ranges between 1770 m a.s.l. at the confluence with the Sutlej River (Sangewar et al., 2001; Kumar and Gupta, 2001) and 6400 m a.s.l. in the area of Rangrik Rang (Fig. 2). The present tree line is situated around 3800–3900 m a.s.l. (Ranhotra and Bhattacharyya, 2010). At present more than 10 villages exist in the Baspa Valley, with Chitkul the highest village at 3450 m.

The two ages from the uppermost lake fill at location 2, at 2650 m a.s.l. originate from a coaly layer and large coal particles and gave 5072 ± 205 cal yr BP and 5181 ± 134 cal yr BP, respectively (Section 4.4, Figs. 5 and 10). Another charcoal layer nearby from location 3, 2646 m a.s.l., with a radiocarbon age of 2156 ± 152 cal yr BP is sandwiched between fluvial gravel of the palaeo-lake topset below and alluvial fan sediments above (Figs. 5, and 6c, Table 1).

Coal particles and the charcoal layers (Figs. 6c, and 10) could be explained by accidental fires caused by lightning, but in this environment thunderstorms usually are accompanied by torrential rains. Especially the accumulation of two charcoal layers and a piece of charcoal within 0.6 m of sediments at location 2 (Fig. 10) is difficult to explain by natural fires, because no charcoal has been found in the palaeo-lake deposits below. In support of this interpretation Chakraborty et al. (2006) found a concentration of charcoal in their lake sediments 4519 ± 56 to 1800 ± 64 uncal yr. Therefore, natural fires cannot be excluded, but human induced fires seem more likely (Meyer et al., 2009; Kaiser et al., 2009). The ages from the top of Sangla palaeo-lake are only slightly younger than charcoal layers from Lunana (Bhutan), 4745 ± 250 and 4680 ± 155 cal yr BP, which have been interpreted as indications for human presence there (Meyer et al., 2009). However the Lunana ages are situated around 3700–4000 m a.s.l. (Meyer et al., 2009) compared to 2650 m a.s.l. of the charcoal in this study. The ages of the two charcoal samples from the Baspa Valley are also quite similar to ages between 5700 and 5400 cal yr BP when Miehe et al. (2009) observe an abrupt decline of *Pinus* forests in many high altitude areas from the Hindukush to northern central Nepal, probably linked to woodland clearance for farmland and pasture.

Therefore the charcoal layers and charcoal pieces may represent one of the oldest evidences for human presence in the Baspa Valley during Neolithic time. Especially the surrounding of Sangla village at the rim of the palaeo-lake, in a quite open section of the Baspa Valley, might have been an advantage location for early settlement (see also Weidinger et al., 2002; Hewitt, 2011). The pollen of sample ED00/15 from this level show an abundance of herbaceous and grassy vegetation, which may reflect forest clearance for pasture.

6. Conclusions

The early-middle Holocene Sangla palaeo-lake is a very rare example of mass movement-dammed lake that has been filled completely and thus represents an exceptional archive for more than 3000 years of erosion and sedimentation processes in a Himalayan catchment. The special location of the Baspa II hydro-power plant on top of the Sangla palaeo-lake allowed the exceptional evaluation of the short-term, river load and hydrological from the planning and operational stages of Baspa II with the long-term parameters from the palaeo-lake sediments with the identical catchment.

The Mid-Holocene erosion rates of the Baspa catchment estimated from the volume and duration of deposition of the lake sediments are very similar to the modern erosion rates of the same catchment calculated from modern river gauge data of Baspa II.

The palynomorph flora of the lowest exposed lake levels are characterized by the abundance and diversity of angiosperm trees and shrubs, particularly evergreen Fagaceae, as well as ferns and fern allies, all of which indicate moist and temperate conditions. In contrast the pollen from just above the topset gravels of the lake indicate a drier zonal environment, with abundant of herbaceous and grassy vegetation.

Several charcoal layers and charcoal pieces from the uppermost palaeo-lake levels around 5000 cal yr BP might be related to woodland clearance and they possibly represent one of the oldest evidences for human presence in the Baspa Valley during Neolithic time.

Acknowledgements

Many thanks to Christian Hager, Jean-Claude Vannay, Hanns Peter Schmid, Rasmus Thiede, Gela Landgraf, Esther Hintersberger, Manfred Strecker and Ramón Arrowsmith for support and discussion in the field. Ingrid Jüttner carried out elaborative investigations on diatoms. This paper benefitted greatly from openly shared ideas and data of Wolfgang Frank and Om Bhargava. Michael Meyer contributed greatly to aspects concerning the settlement history and Benjamin Huet helped with volume calculation. The constructive comments by two anonymous reviewers are kindly acknowledged. Many thanks to Walter Kutschera and Eva Maria Wild from the Institute for Isotope Research and Nuclear Physics, University of Vienna for ^{14}C dating of organic samples. Financial support was provided by the FWF (*Fonds zur Förderung der wissenschaftlichen Forschung*) through project P-14129-Geo.

References

Andermann, C., Crave, A., Gloaguen, R., Davy, Ph., Bonnet, St., 2012. Connecting source and transport: suspended sediments in the Nepal Himalayas. Earth Planet. Sci. Lett. 351–352, 158–170.

Bali, R., Nawaz Ali, S., Agarwal, K.k., Kumar Rastogi, S., Krishna, K., Srivastava, P., 2013. Chronology of late Quaternary glaciation in the Pindar valley, Alaknanda basin, Central Himalaya (India). J. Asian Earth Sci. 66, 224–233.

Barnard, P.L., Owen, L.A., Finkel, R.C., 2004. Style and timing of glacial and paraglacial sedimentation in a monsoon-influenced high Himalayan environment, the upper Bhagirathi Valley, Garhwal Himalaya. Sed. Geol. 165, 199–221.

Beaumont, C., Jamieson, R.A., Nguyen, M.H., Lee, B., 2001. Himalayan tectonics explained by extrusion of a low-viscosity crustal channel coupled to focused surface denudation. Nature 414, 738–742.

Baspa II, 2004. Baspa-II Hydroelectric Project: General project information. <http://members.rediff.com/psr/baspa.htm> (accessed 20.02.04).

Bhargava, O.N., Bassi, U.K., 1998. Geology of Spiti-Kinnaur Himachal Himalaya. Geol. Surv. India Memoirs 124, 1–210.

Bookhagen, B., Burbank, D.W., 2010. Toward a complete Himalayan hydrological budget: spatiotemporal distribution of snowmelt and rainfall and their impact on river discharge. J. Geophys. Res. 115, F03019. http://dx.doi.org/10.1029/2009JF001426.

Bookhagen, B., Thiede, R.C., Strecker, M.R., 2005a. Late quaternary intensified monsoon phases control landscape evolution in the northwest Himalaya. Geology 33 (2), 149–152.

Bookhagen, B., Thiede, R.C., Strecker, M.R., 2005b. Abnormal Monsoon years and their control on erosion and sediment flux in the high, arid northwest Himalaya. Earth Planet. Sci. Lett. 231, 131–146.

Brantingham, P.J., Xing, G., Olsen, J.W., Haizhou, M., Rhode, D., Haiying, Z., Madsen, D.B., 2007. A short chronology for the peopling of the Tibetan Plateau. Dev. Quat. Sci. 9, 129–150.

Bronk Ramsey, C., 2010. OxCal Program, v. 4.1.7, Radiocarbon Accelerator Unit, University of Oxford, UK, <http://c14.arch.ox.ac.uk/embed.php?File=oxcal.html> (accessed 04.06.12).

Bull, W.B., 2009. Tectonically Active Landscapes. Wiley-Blackwell, Oxford, 326 pp..

Burbank, D.W., Bookhagen, B., Gabet, E.J., Putkonen, J., 2012. Modern climate and erosion in the Himalaya. C.R. Geosci. 344, 610–626.
Burchfield, B.C., Zhiliang, C., Hodges, K.V., Yuping, L., Royden, L.H., Changrong, D., Jiene, X., 1992. The South Tibetan Detachment System, Himalayan Orogen. Extension contemporaneous with and parallel to shortening in a collisional mountain belt. Geological Society of America Special Paper 269, 41 pp.
Chakraborty, S., Bhattacharya, S.K., Ranhotra, P.S., Bhattacharya, A., Bhushan, R., 2006. Palaeoclimatic scenario during Holocene around Sangla valley, Kinnaur northwest Himalaya based on multi proxy records. Curr. Sci. 91 (6), 777–782.
Chamley, H., 1989. Clay Sedimentology. Springer, Berlin, 623 pp..
Collett, H., 1902. Flora Simlensis; A Handbook of the Flowering Plants of Simla and the Neighbourhood. Thacker, Spink & Co., Simla, 652 pp..
Costa, J.E., Schuster, R.L., 1988. The formation and failure of natural dams. Geol. Soc. Am. Bull. 100, 1054–1068.
Costa, J.E., Schuster, R.L., 1991. Documented historical landslide dams from around the World. U.S. Geological Survey Open-File, Report 91–239, 486 pp.
Dahlen, F.A., Suppe, J., 1988. Mechanics, growth, and erosion of mountain belts. In: Clark, S.P., Burchfiel, B.C., Suppe, J. (Eds.), Processes in Continental Lithospheric Deformation. Geological Society of America Special Paper 218, pp. 161–178.
Draganits, E., 2000. The Muth Formation in the Pin Valley (Spiti, N-India): Depositional Environment and Ichnofauna of a Lower Devonian Barrier Island System. PhD-thesis, University of Vienna, 144 pp. <http://othes.univie.ac.at/158/1/Draganits_2000_Dissertation_Himalaya.pdf> (accessed 04.08.13).
Draganits, E., Schlaf, J., Grasemann, B., Argles, T., 2008. Giant submarine landslide grooves in the Neoproterozoic/Lower Cambrian Phe Formation, northwest Himalaya: mechanisms of formation and palaeogeographic implications. Sed. Geol. 205, 126–141.
Draganits, E., Grasemann, B., Janda, C., Hager, C., Preh, A., 2014. 300 MW Baspa II – India's largest private hydroelectric facility on top of a rock avalanche-dammed palaeo-lake (NW Himalaya): regional geology, tectonic setting and seismicity. Eng. Geol. 169, 14–29.
Emmett, W.W., 2010, Observations of Bedload Behavior in Rivers and Their Implications for Indirect Methods of Bedload Measurement. U.S. Geological Survey Scientific Investigations Report 2010-5091, 159–170. <http://pubs.usgs.gov/sir/2010/5091/papers/Emmett.pdf> (accessed 01.08.13).
Gabet, E.J., Burbank, D.W., Pratt-Sitaula, B., Putkonen, J., Bookhagen, B., 2008. Modern erosion rates in the High Himalayas of Nepal. Earth Planet. Sci. Lett. 267, 482–494.
Gadgil, S., 2003. The Indian monsoon and its variability. Annu. Rev. Earth Planet. Sci. 31, 429–467.
Hager, C., 2003. Out-of-sequence extrusion in the Sutlej Valley (NW-Himalaya). unpubl. Diploma thesis, University of Vienna, Vienna, 91 pp.
Hauck, M.L., Nelson, K.D., Brown, L.D., Zhao, W., Ross, A.R., 1998. Crustal structure of the Himalayan orogen at ~90° east longitude from project indepth deep reflection profiles. Tectonics 17, 481–500.
Hewitt, K., 2011. Rock avalanche dams on the Trans Himalayan upper Indus streams: a survey of late Quaternary events and hazard-related characteristics. In: Evans, S.G., Hermanns, R.L., Strom, A., Scarascia-Mugnozza, G. (Eds.), Natural and Artificial Rockslide Dams. Lecture Notes in Earth Sciences 133. Springer, Heidelberg, pp. 177–204.
Hinderer, M., 2001. Late Quaternary denudation of the Alps, valley and lake fillings and modern river loads. Geodin. Acta 14, 231–263.
Hintersberger, E., Thiede, R., Strecker, M., 2011. The role of extension during brittle deformation within the NW Indian Himalaya. Tectonics 30, TC3012. http://dx.doi.org/10.1029/2010TC002822.
Hodges, K.V., 2000. Tectonics of the Himalaya and southern Tibet from two perspectives. Geol. Soc. Am. Bull. 112, 324–350.
Jarvis A., Reuter, H.I., Nelson, A., Guevara, E., 2008. Hole-filled seamless SRTM data V4, International Centre for Tropical Agriculture (CIAT), <http://www.srtm.csi.cgiar.org> (accessed 22.07.13).
JHPL (Jaiprakash Hydro-Power Limited), 2004. Baspa II: Project profile. <http://www.jhpl.com/baspa-projectprofile.htm> (accessed 02.03.12).
Kaiser, K., Opgenoorth, L., Schoch, W.H., Miehe, G., 2009. Charcoal and fossil wood from palaeosols, sediments and artificial structures indicating Late Holocene woodland decline in southern Tibet (China). Quatern. Sci. Rev. 28 (15–16), 1539–1554.
Korup, O., 2011. Rockslide and rock avalanche dams in the Southern Alps, New Zealand. In: Evans, S.G., Hermanns, R.L., Strom, A., Scarascia-Mugnozza, G. (Eds.), Natural and Artificial Rockslide Dams. Lecture Notes in Earth Sciences 133. Springer, Heidelberg, pp. 123–145.
Korup, O., Strom, A.L., Weidinger, J.T., 2006. Fluvial response to large rock-slope failures: examples from the Himalayas, the Tien Shan, and the Southern Alps in New Zealand. Geomorphology 78, 3–21.
Kulkarni, A.V., 2007. Effect of global warming on the Himalayan cryosphere. Jalvigyan Sameeksha 22, 93–108.
Kulkarni, A.V., Alex, S., 2003. Estimation of recent glacial variations in Baspa Basin using remote sensing technique. J. Indian Soc. Remote Sens. 31 (2), 81–90.
Kulkarni, A.V., Rathore, B.P., Alex, S., 2004. Monitoring of glacial mass balance in the Baspa basin using accumulation area ratio method. Curr. Sci. 86 (1), 185–190.
Kumar, S., Gupta, S.K., 2001. Pre-historic blockades of Baspa River: their origin and geotechnical significance. Symposium on Snow, ice and glaciers; a Himalayan perspective, Lucknow, India, 9-11 March 1999, Geological Survey of India Special Publication Series 53, pp. 303–308.
Mackey, B.H., Roering, J.J., Lamb, M.P., 2011. Landslide-dammed paleolake perturbs marine sedimentation and drives genetic change in anadromous fish. Proc. Nat. Acad. Sci. USA 108 (47), 18905–18909.
Meyer, M.C., Hofmann, C., Gemmell, A.M.D., Haslinger, E., Häusler, H., Wangda, D., 2009. Holocene glacier fluctuations and migration of Neolithic yak pastoralists into the high valleys of northwest Bhutan. Quatern. Sci. Rev. 28, 1217–1237.
Miehe, G., Miehe, S., Schlütz, F., 2009. Early human impact in the forest ecotone of southern High Asia (Hindu Kush, Himalaya). Quatern. Res. 71, 255–265.
Molnar, P., 2009. The state of interactions among tectonics, erosion, and climate: a polemic. GSA Today 19 (7), 44–45.
Molnar, P., England, P., 1990. Late Cenozoic uplift of mountain ranges and global climate change: chicken or egg? Nature 346, 29–34.
Montenat, C., Barrier, P., d'Estevou, Ott, Hibsch, C., 2007. Seismites: an attempt at critical analysis and classification. Sed. Geol. 196, 5–30.
Owen, L.A., 1998. Timing and style of Glaciation in the Himalaya. Himalayan Geol. 19, 39–47.
Owen, L.A., Finkel, R.C., Caffee, M.W., 2002. A note on the extent of glaciation throughout the Himalaya during the global Last Glacial Maximum. Quatern. Sci. Rev. 21, 147–157.
Owen, L.A., Gualtieri, L., Finkel, R.C., Caffee, M.W., Benn, D.I., Sharma, M.C., 2001. Cosmogenic radionuclide dating of glacial landforms in the Lahul Himalaya, northern India: defining the timing of Late Quaternary glaciation. J. Quat. Sci. 16 (6), 555–563.
Polunin, O., Stainton, A., Farrer, A., 1999. Flowers of the Himalaya. Oxford India paperbacks, Delhi, 580 pp..
Pratt-Sitaula, B., Garde, M., Burbank, D.W., Oskin, M., Heimsath, A., Gabet, E., 2007. Bedload-to-suspended load ratio and rapid bedrock incision from Himalayan landslide-dam lake record. Quatern. Res. 68, 111–120.
Prell, W.L., Kutzbach, J.E., 1987. Monsoon variability over the past 150,000 years. J. Geophys. Res. 92, 8411–8425.
Putkonen, J.K., 2004. Continuous snow and rain data at 500–4400 m altitude near Annapurna, Nepal, 1999–2001. Arct. Antarct. Alp. Res. 36, 244–248.
Ranhotra, P.S., Bhattacharyya, A., 2010. Holocene palaeoclimate and glacier fluctuations within Baspa Valley, Kinnaur, Himachal Pradesh. J. Geol. Soc. India 75, 527–532.
Rhode, D., Madsen, D.B., Brantingham, P.J., Dargye, T., 2007. Yaks, yak dung, and prehistoric human habitation of the Tibetan Plateau. Dev. Quat. Sci. 9, 205–224.
Sangewar, C.V., Shukla, S.P., 2001. Glacier inventory of Beas and Satluj basins in the districts of Kullu, Mandi, Rampur Bushar and Kinnaur, Himachal Pradesh. Symposium on Snow, ice and glaciers; a Himalayan perspective, Lucknow, India, 9-11 March 1999, Geological Survey of India Special Publication Series 53, pp. 257–264.
Sangewar, C.V., Singh, R.K., Siddiqui, M.A., 2001. Morphometric analysis vis-à-vis geomorphology of the Baspa Basin, District Kinnaur, Himachal Pradesh. Symposium on Snow, ice and glaciers; a Himalayan perspective, Lucknow, India, 9-11 March 1999, Geological Survey of India Special Publication Series 53, pp. 265–273.
Scherler, D., Bookhagen, B., Strecker, M.R., von Blanckenburg, F., Rood, D., 2010. Timing and extend of late Quaternary glaciation in the western Himalaya constrained by ^{10}Be moraine dating in Garhwal, India. Quatern. Sci. Rev. 29, 815–831.
Schultz, L.G., 1964. Quantitative interpretation of mineralogical composition from X-ray and chemical data for the Pierre shale. US Geological Survey Professional Paper, 391-C, U.S. Government Printing Office, Washington, 31 pp.
Schuster, R.L., Costa, J.E., 1986. A perspective on landslide dams. In: Schuster, R.L. (Ed.), Landslide Dams: Processes, Risks, and Mitigation. Proceedings of a Session Sponsored by the Geotechnical Engineering Division of the American Society of Civil Engineers in conjunction with the ASCE Convention in Seattle, Washington April 7, 1986, Geotechnical Special Publication 3, American Society of Civil Engineers, New York, pp. 1–20.
Sharma, M.C., Owen, L.A., 1996. Quaternary glacial history of the Garwhal Himalaya, India. Quatern. Sci. Rev. 15, 335–365.
Shrestha, B.P., 1989. Forest Plants of Nepal. Educational Enterprise, Lalitpur, 216 pp..
Shukla, U.K., Kotlia, B.S., Mathur, P.D., 2002. Sedimentation pattern in a trans-Himalayan Quaternary lake at Lamayuru (Ladakh), India. Sed. Geol. 148, 405–424.
Singh, S., Jain, A.K., 2001. Paleoseismicity: geological evidence along the Kaurik-Chango Fault Zone and other related areas in Lahaul-Spiti and Ladakh Himalaya. In: Varma, O.P. (Ed.), Seismicity. Research Highlights in Earth System Science, Department of Science and Technology Special Publications, vol. 2, Indian Geological Congress, pp. 205–225.
Singh, B.P., Kumar, R., Kalsotra, B.L., 2001. Suspended and dissolved flux in the Baspa River, Kinnaur District, Himachal Pradesh; evaluation of weathering and erosion. National symposium: Role of earth sciences in integrated development and related societal issues, Lucknow, India, 2–4 November 2001, Geological Survey of India Special Publication Series 65(3), 31–35.
Srikantia, S.V., Bhargava, O.N., 1998. Geology of Himachal Pradesh. Geological Society of India, Bangalore, 406 pp..
Stainton, J.D.A., 1972. Forests of Nepal. London Camelot Press, p. 180.
Thiede, R.C., Ehlers, T.A., 2013. Large spatial and temporal variations in Himalayan denudation. Earth Planet. Sci. Lett. 371–372, 278–293.
Treydte, K.S., Schleser, G.H., Helle, G., Frank, D.C., Winiger, M., Haug, G.H., Esper, J., 2006. The twentieth century was the wettest period in northern Pakistan over the past millennium. Nature 440, 1179–1182.
Tripathi, K., Sen, K., Dubey, A., 2012. Modification of fabric in pre-Himalayan granitic rocks by post-emplacement ductile deformation: insights from microstructures, AMS, and U-Pb geochronology of the Paleozoic Kinnaur Kailash Granite and associated Cenozoic leucogranites of the South Tibetan Detachment zone, Himachal High Himalaya. Int. J. Earth Sci. 101, 761–772.

Trivedi, A., Chauhan, M.S., 2009. Holocene vegetation and climate fluctuations in Northwest Himalaya, based on pollen evidence from Surinsar Lake, Jammu Region, India. J. Geol. Soc. India 74, 402–412.

Vannay, J.-C., Grasemann, B., 2001. Himalayan inverted metamorphism and syn-convergence extension as a consequence of a general shear extrusion. Geol. Mag. 138, 253–276.

Vannay, J.-C., Grasemann, B., Rahn, M., Frank, W., Carter, A., Baudraz, V., Cosca, M., 2004. Miocene to Holocene exhumation of metamorphic crustal wedges in the NW Himalaya: evidence for tectonic extrusion coupled to fluvial erosion. Tectonics 23. http://dx.doi.org/10.1029/2002TC001429.

Verstraeten, G., Poesen, J., 2001. Variability of dry sediment bulk density between and within retention ponds and its impact on the calculation of sediment yields. Earth Surf. Proc. Land. 26, 375–394.

Weidinger, J.T., Wang, J., Ma, N., 2002. The earthquake-triggered rock avalanche of Cui Hua, Qin Ling Mountains, P.R. of China – the benefits of a lake-damming prehistoric natural disaster. Quatern. Int. 93–94, 207–214.

Weidinger, J.T., 2011. Stability and life span of landslide dams in the Himalayas (India, Nepal) and the Qin Ling Mountains (China). In: Evans, S.G., Hermanns, R.L., Strom, A., Scarascia-Mugnozza, G. (Eds.), Natural and Artificial Rockslide Dams. Lecture Notes in Earth Sciences 133. Springer, Heidelberg, pp. 243–277.

Whipp, D.M.J., Ehlers, T.A., Blythe, A.E., Huntington, K.W., Hodges, K.V., Burbank, D.W., 2007. Plio-Quaternary exhumation history of the central Himalaya: 2. Thermokinematic model of the thermochronometer exhumation. Tectonics 26, TC3003. http://dx.doi.org/10.1029/2006TC001991.

Whipple, K.X., 2009. The influence of climate on the tectonic evolution of mountain belts. Nat. Geosci. 2 (2), 97–104.

Whittaker, A.C., 2012. How do landscapes record tectonics and climate? Lithosphere 4 (2), 160–164.

Willett, S.D., Hovius, N., Brandon, M.T., Fisher, D.M. (Eds.), 2006. Tectonics, Climate and Landscape Evolution. Geological Society of America Special Papers 398, 434 p.

Wulf, H., Bookhagen, B., Scherler, D., 2010. Seasonal precipitation gradients and their impact on fluvial sediment flux in the Northwest Himalaya. Geomorphology 118, 13–21.

Wulf, H., Scherler, D., Bookhagen, B., 2012. Climatic and geologic controls on suspended sediment flux in the Sutlej River Valley, Western Himalaya. Hydrol. Earth Syst. Sci. Discuss. 9, 541–594.

Wünnemann, B., Demske, D., Tarasov, P., Kotlia, B.S., Reinhardt, C., Bloemendal, J., Diekmann, B., Hartmann, K., Krois, J., Riedel, F., Arya, N., 2010. Hydrological evolution during the last 15 kyr in the Tso Kar lake basin (Ladakh, India), derived from geomorphological, sedimentological and palynological records. Quatern. Sci. Rev. 29, 1138–1155.